DRF Codes: Deep SNR-Robust Feedback Codes

Mahdi Boloursaz Mashhadi, Deniz Gündüz, Alberto Perotti, and Branislav Popovic

***Abstract*— We present a new deep-neural-network (DNN) based error correction code for fading channels with noisy channel output feedback, called deep SNR-robust feedback (DRF) code. At the encoder, parity symbols are generated by a long short term memory (LSTM) network based on the message as well as the past forward channel outputs observed by the transmitter in a noisy fashion. The decoder uses a bi-directional LSTM architecture along with a signal to noise ratio (SNR)-aware attention module. The proposed code overcomes two major shortcomings of the previously proposed DNN-based codes over channels with noisy channel output feedback: (i) SNR-aware attention mechanism at the decoder enables reliable application of the same trained DNN over a wide range of SNR values; (ii) curriculum training with batch-size scheduling is used to speed up and stabilize training while improving the SNR-robustness of the resulting code. We show that the DRF codes significantly outperform state-of-the-art in terms of both the SNR-robustness and the error rate in additive white Gaussian noise (AWGN) channels with feedback. In fading channels with perfect phase compensation at the receiver, DRF codes learn to efficiently exploit the knowledge of the instantaneous fading amplitude (which is available to the encoder through feedback) to reduce the overhead and complexity associated with channel estimation at the decoder.**

***Index terms*—** Communication with feedback, channel coding, LSTM, attention neural networks, curriculum training.

I. Introduction

Most wireless communication systems incorporate some form of feedback from the receiver to the transmitter. Although feedback does not improve the Shannon capacity of a channel [1], it can significantly boost the reliability at finite block-lengths [2]–[4]. Codes that make full use of feedback can potentially achieve improved performance as predicted in [4]. However, the design of reliable codes for channels with feedback has been a long-standing and notoriously difficult problem. Several coding schemes for channels with feedback have been proposed in the past [2], [5]–[8]; however, known solutions either do not approach the performance predicted in [4], or introduce unaffordable complexity. These schemes are also extremely sensitive to both the precision of the numerical computations and the noise in the feedback channel [3]. It has been proven that with noisy output feedback, linear coding schemes fail to achieve any positive rate [9]. This is especially troubling since all practical codes are linear and linear codes are known to achieve capacity without feedback [10], and boost the error performance significantly in the case of noiseless feedback [2]. For the noisy feedback case, considerable improvements have been achieved using non-linear modulo operations [11].

More recently, some progress has been made by applying machine learning (ML) techniques, where channel decoding is regarded as a classification task, and the encoder and decoder, implemented as deep neural network (DNN) architectures, are jointly trained in a data-driven fashion [12]–[14]. In [12], the authors propose Deepcode for communication with feedback, consisting of a recurrent neural network (RNN) encoder architecture along with a two-layer bi-directional gated recurrent unit (GRU) decoder architecture, which are trained jointly on a dataset of random input/output realizations of the channel. In [13], a convolutional neural network (CNN) encoder/decoder architecture with interleaving is used. In [14], deep extended feedback (DEF) codes are introduced, which improve the error correction capability in [12] by an extended feedback mechanism that introduces longer range dependencies within the code blocks. These DNN-based codes achieve lower error rates in comparison with traditional codes (e.g. Turbo, LDPC, and Polar codes that do not exploit the feedback, as well as the Schalkwijk–Kailath scheme [2] with a low resolution feedback), over an additive white Gaussian noise (AWGN) channel with output feedback at the typical code rate of $r = 1/3$ and relatively short block length of $L = 50$ [12]–[14].

Despite their significant performance, DNN-based codes are very sensitive to the mismatch between the actual channel signal to noise ratio (SNR) and the SNR value that the code is trained for, which limits their application in practical communication systems with time-varying SNR values. In this paper, we propose **D**eep SNR-**R**obust **F**eedback (DRF) codes for fading channels with noisy output feedback, which overcome the above-mentioned limitation of DNN-based channel codes. The DRF encoder transmits a message followed by a sequence of parity symbols, which are generated by a long short term memory (LSTM) architecture based on the message as well as the delayed past forward channel outputs observed by the encoder through a noisy feedback channel. The decoder uses a bi-directional LSTM architecture along with a SNR-aware attention [15], [16] network to decode the message. The major contributions of this paper can be summarized as follows:

- We propose an attention mechanism that enables SNR-aware decoding of the DRF code, thereby considerably improving its robustness in realistic time-varying channels, where there may be a considerable mismatch between the training SNR and the instantaneous channel SNR. For fading channels, in which the instantaneous SNR may be varying on each transmitted codeword (slow fading) or symbol (fast fading), we show that the proposed DRF codes learn to efficiently exploit the Channel State Information (CSI), which is available to the encoder through feedback, and no further improvement is possible by providing the CSI to the decoder.
- We propose a training approach with SNR scheduling and batch-size adaptation. We start the training at low SNR values with a small batch-size, and gradually increase the SNR and the batch-size along the training epochs according to a schedule. The proposed training approach improves the SNR-robustness of the resulting code and speeds up the training. The DRF codes with the proposed training approach not only achieve considerable SNR-robustness, but also improve the error rate over Deepcode [12] roughly by an order of magnitude.

The rest of this paper is organized as follows. In Section II, we present the feedback channel model considered in this paper. In Section III, we provide the DNN architectures for the DRF encoder and decoder. In Section IV, we present our proposed training technique. Section V presents the simulation results, and Section VI concludes the paper.

II. System Model

Fig. 1 illustrates the canonical fading channel with passive noisy output feedback considered in this paper. Perfect phase compensation

M. Boloursaz Mashhadi is with the 5GIC & 6GIC, Institute for Communication Systems (ICS), University of Surrey, UK. D. Gündüz is with the Dept. of Electrical and Electronic Eng., Imperial College London, UK. A. Perotti and B. Popovic are with the Radio Transmission Technology Laboratory, Huawei Technologies Sweden.

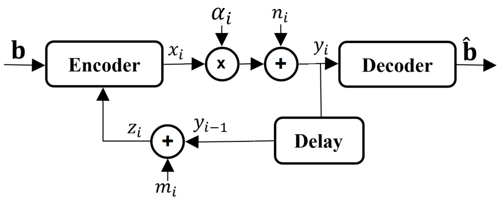

Fig. 1: Fading channel with noisy channel output feedback.

at the receiver is assumed resulting in a real-valued magnitude fading channel. We have $y_i = \alpha_i x_i + n_i$, where x_i and y_i denote the channel input and output symbols, respectively, α_i is the channel fading coefficient, n_i is the independent and identically distributed (i.i.d.) Gaussian noise term, i.e., $n_i \sim \mathcal{N}(0, \sigma_n^2)$. We will assume that the channel fading coefficient comes from a prescribed distribution. We consider both slow and fast fading scenarios, where the fading coefficient remains constant on each codeword in the former but takes i.i.d. random values on each symbol for the latter case. The channel output is assumed to be available at the encoder with a unit time delay via an independent AWGN feedback channel. At time i, the encoder has a noisy view of what was received at the decoder (in the past by one unit time) $z_i = y_{i-1} + m_i$, where m_i is an i.i.d. Gaussian noise term, i.e., $m_i \sim \mathcal{N}(0, \sigma_m^2)$. We call this a *passive* output feedback, as unlike in [11], the decoder cannot apply any coding or other type of transformation on its received signal y_i before feeding it back to the encoder. The encoder can use the feedback symbol to sequentially and adaptively decide what to transmit as the next symbol. Therefore, channel input x_i at time instant i depends not only on the message $\mathbf{b} \in \{0,1\}^K$, but also on the past feedback symbols. The encoder maps the message $\mathbf{b} \in \{0,1\}^K$ onto the codeword $\mathbf{x} = [x_1, \ldots, x_L]^T$, where L is the block length and K is the message length. The decoder maps the received codeword $\mathbf{y} = [y_1, \ldots, y_L]^T$ into the decoded message $\hat{\mathbf{b}} \in \{0,1\}^K$, where $r = K/L$ is the rate of the code. The block error rate (BLER) is given by $\text{BLER} = Pr\{\hat{\mathbf{b}} \neq \mathbf{b}\}$. Similarly, the bit error rate (BER) is given by $\text{BER} = 1/K \sum_{k=1}^{K} Pr\{\hat{b}_k \neq b_k\}$, where b_k and $\hat{b}_k$ denote the k'th bit of the transmitted and decoded messages, respectively. We assume an average power constraint on the channel input, i.e., $\frac{1}{L}\mathbb{E}[\|\mathbf{x}\|^2] \leq 1$, where the expectation is over the randomness in the information bits, the randomness in the noisy feedback symbols $[z_1, \ldots, z_L]^T$ and any other randomness in the encoder. We denote the forward and feedback channel SNR values by $\rho = 1/\sigma_n^2$ and $\eta = 1/\sigma_m^2$, respectively.

III. Encoder/Decoder Architectures

A major limitation of the existing DNN-based code designs in [12]–[14] is their dependence on the channel SNR. That is, the encoder-decoder pairs are trained jointly for a specific SNR value. This means that, to be able to use these codes in practice, we will have to train and store a different DNN pair for different ranges of SNR values, which significantly limits their practical use in realistic channels with varying SNR. On the other hand, in conventional channel codes, the encoder depends only on the transmit power constraint, and the decoder uses the same decoding algorithm for all SNR values after converting the channel outputs into likelihood values depending on the channel SNR. Accordingly, a major goal of our paper is to implement a similar approach for DNN-based code design. This is achieved in this paper by incorporating an attention mechanism into the decoder of our proposed DRF code. This will allow us to train and store a single DNN, which can be used for all SNR values. Apart from this, we design the DRF code for fading channels with feedback, when the instantaneous channel SNR may change over time. This is different from the previous works that

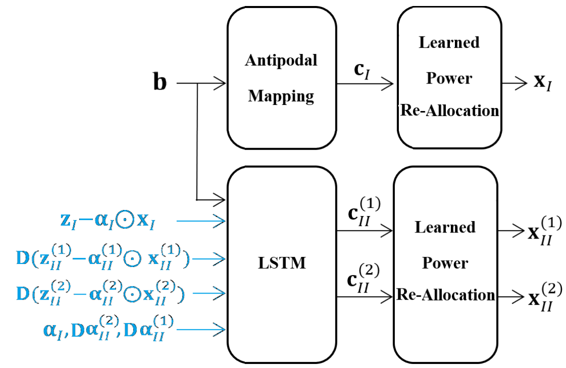

(a) Encoder architecture.

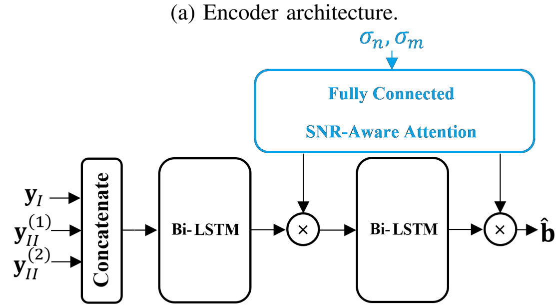

(b) Decoder architecture.

Fig. 2: The block diagram of the proposed DRF code structure, (a) encoder, (b) decoder. The novelties of the DRF encoder and decoder architectures are shown in blue for emphasis.

consider the simple AWGN channel with feedback [12]–[14]. Fig. 2 depicts our proposed DRF encoder and decoder architectures for a rate $r = 1/3$ code (the architecture could be easily generalized to all rates $r = 1/q$ with q being any positive integer greater than 1).

A. Encoder

Fig. 2a illustrates the encoder architecture. Encoding is a two-phase process: in phase I, vector $\mathbf{b} = [b_1, \ldots, b_K, 0]^T$ consisting of the message bits padded by a zero is transmitted over the channel by an antipodal mapping, i.e., $\mathbf{c}_I = 2\mathbf{b} - 1$. Zero padding is applied to mitigate the increasing error rate effects on the last few bits of the block as suggested in [12]. During phase II, the encoder uses a 1-layer LSTM network, including $K+1$ LSTM units to generate two sets of parity bits, i.e., $\mathbf{c}_{II}^{(1)}$ and $\mathbf{c}_{II}^{(2)}$, based on the observations of channel noise and fading in phase I and the delayed noise and fading in phase II on each of the two sets of parity symbols. We use single directional LSTM units due to the causality constraint enforced by the channel model. The LSTM activation is hyperbolic tangent, i.e., $\tanh(x) = \frac{e^x - e^{-x}}{e^x + e^{-x}}$, while the output activation function is sigmoid, i.e., $\text{sigmoid}(x) = \frac{1}{1+e^{-x}}$. The resulting code block transmitted over the channel is $\mathbf{x} = [\mathbf{x}_I^T, \mathbf{x}_{II}^{(1)T}, \mathbf{x}_{II}^{(2)T}]^T = [x_1, \ldots, x_{3K+3}]^T$, where $\mathbf{x}_I = \mathcal{P}\{\mathbf{c}_I\} = [x_1, x_2, \ldots, x_{K+1}]^T$, $\mathbf{x}_{II}^{(1)} = \mathcal{P}\{\mathbf{c}_{II}^{(1)}\} = [x_{K+2}, x_{K+3}, \ldots, x_{2K+2}]^T$, and $\mathbf{x}_{II}^{(2)} = \mathcal{P}\{\mathbf{c}_{II}^{(2)}\} = [x_{2K+3}, x_{2K+4}, \ldots, x_{3K+3}]^T$. Here, $\mathcal{P}\{\cdot\}$ denotes a learned power re-allocation layer to balance the error over the whole block as suggested in [12].

The encoder estimates the forward channel from observations of the feedback. It knows the transmitted symbol x_i and observes the corresponding feedback symbol $z_i = \alpha_{i-1}x_{i-1} + n_{i-1} + m_i$ with a single delay, from which it can estimate the CSI α_{i-1}. The estimate of the CSI, denoted by $\hat{\alpha}_{i-1}$, is then input to the encoder. In the fast fading scenario, where the fading coefficient takes random i.i.d. realizations on each symbol, the linear minimum mean square error (LMMSE) estimate of the channel gain is calculated by

$$\hat{\alpha}_i = \frac{x_{i-1}\mathrm{var}(\alpha)}{|x_{i-1}|^2\mathrm{var}(\alpha)+\sigma_n^2+\sigma_m^2} z_i + \frac{\sigma_n^2+\sigma_m^2}{|x_{i-1}|^2\mathrm{var}(\alpha)+\sigma_n^2+\sigma_m^2}\mathbb{E}[\alpha], \quad (1)$$

where $\mathbb{E}[\alpha]$ and $\mathrm{var}(\alpha)$ denote the expected value and variance of the fading coefficient, respectively. In a slow fading scenario, the fading coefficient is fixed over the whole codeword, i.e., for the considered rate $r = 1/3$ code with a single bit zero padding we have $\alpha_1 = \cdots = \alpha_{3K+3} = \alpha$. The fading coefficient α takes random i.i.d. realizations over different codewords, and the transmitter uses the causal vectors $\mathbf{z}_i = [z_1, \ldots, z_i]^T$ and $\mathbf{x}_i = [x_1, \ldots, x_i]^T$ to calculate the LMMSE channel estimate as

$$\begin{aligned}\hat{\alpha} &= \mathrm{var}(\alpha)\mathbf{x}_{i-1}^T(\mathrm{var}(\alpha)\mathbf{x}_{i-1}\mathbf{x}_{i-1}^T + \sigma_n^2 I + \sigma_m^2 I)^{-1}\mathbf{z}_i \quad (2)\\ &+ \mathbb{E}[\alpha](1 - \mathrm{var}(\alpha)\mathbf{x}_{i-1}^T(\mathrm{var}(\alpha)\mathbf{x}_{i-1}\mathbf{x}_{i-1}^T + \sigma_n^2 I + \sigma_m^2 I)^{-1}\mathbf{x}_{i-1}),\end{aligned}$$

in which I is the identity matrix. In (1), (2), knowledge of $\mathbb{E}[\alpha]$ and $\mathrm{var}(\alpha)$ at the transmitter is assumed.

The causal CSI available at the encoder is fed into the LSTM units to cope with channel uncertainty due to fading. To this end, we concatenate the vector of instantaneous channel fading coefficients in phase I, i.e. $\alpha_I = [\alpha_1, \ldots, \alpha_{K+1}]^T$, and the causal fading coefficient in phase II i.e. $\mathbf{D}\alpha_{II}^{(1)} = [0, \alpha_{K+2}, \ldots, \alpha_{2K+1}]^T$, and $\mathbf{D}\alpha_{II}^{(2)} = [0, \alpha_{2K+3}, \ldots, \alpha_{3K+2}]^T$, and feed into the LSTM units at the encoder ($\mathbf{D}$ denotes a single delay, see Fig. 2a). We also provide estimates of the noise in the forward and feedback channels to the encoder, i.e. $\mathbf{z}_I - \alpha_I \odot \mathbf{x}_I$, $\mathbf{D}(\mathbf{z}_{II}^{(1)} - \alpha_{II}^{(1)} \odot \mathbf{x}_{II}^{(1)})$, and $\mathbf{D}(\mathbf{z}_{II}^{(2)} - \alpha_{II}^{(2)} \odot \mathbf{x}_{II}^{(2)})$, where $\odot$ denotes element-wise multiplication. For the AWGN case where $\alpha_I = \alpha_{II}^{(1)} = \alpha_{II}^{(2)} = 1$, the corresponding inputs are omitted to avoid unnecessary complexity.

B. Decoder

Fig. 2b illustrates the DRF decoder consisting of a two-layer LSTM architecture (each including $K+1$ LSTM units) and a SNR-aware fully connected attention network. At the decoder, we use bi-directional LSTM layers to exploit long range forward and backward dependencies in the received code block. The phase I and II received signals are concatenated at the decoder and fed to the bi-directional LSTM layers. Each LSTM layer is followed by batch normalization. Similarly to the encoder, the LSTM activation is hyperbolic tangent while the output activation is sigmoid. The bi-directional LSTM layers extract features from the noisy received signals, which are then used for efficient decoding. Note that we use LSTM layers at both the encoder and the decoder, which, according to our observations, considerably reduce the error rate in comparison with simple RNN and GRU layers used in [12]. This is because LSTM layers can better learn long-range dependencies by avoiding the gradient vanishing problem in training long RNN layers [17].

C. SNR-Aware Attention

Another novelty in our decoder architecture is the SNR-aware attention module. An attention mechanism is a vector of importance weights to measure the correlations between a vector of inputs and the target to be predicted. Attention weights are calculated as a parameterized attention function with learnable parameters [15], [16]. We use a two-layer fully connected (FC) attention at the DRF decoder. The idea is to let the attention layers learn how much each bi-LSTM output features should be weighted according to the SNR. Also, by means of the attention module, we explicitly provide the noise standard deviation to the decoder, which enables learning codes that are capable of adaptation to the channel SNR, which in turn allows to use the same trained encoder/decoder weights over a wide range of channel SNR values. Here, the standard deviations of the forward and feedback channel noise are obtained through link-level estimation. The number of attention weights determines the number of neurons at the last FC layer, i.e., $2HK$, where H is the length of the LSTM hidden state (i.e., $H = K$ here) and is multiplied by 2 because the LSTM layer is bi-directional. The total number of FC attention layers and the number of neurons in each intermediate layer are hyperparameters optimized numerically for the best performance.

IV. Training DRF Codes

We denote the i'th training sample by $\mathbf{S}_i = \{\mathbf{b}_i, \alpha_i, \mathbf{n}_i, \mathbf{m}_i\}$, which consists of a random realization of the message $\mathbf{b}_i$, the corresponding realization of the channel fading coefficient α_i, and the forward and feedback noise realizations, $\mathbf{n}_i$ and $\mathbf{m}_i$, respectively. We denote the encoder and decoder functions by $f(\cdot;\theta)$ and $g(\cdot;\psi)$, where θ and ψ are the trainable encoder and decoder parameters. We have, $\hat{\mathbf{b}}_i = g(\alpha_i f(\mathbf{S}_i;\theta) + \mathbf{n}_i;\psi)$. To train the model, we minimize

$$\mathcal{L}(\theta,\psi,\mathcal{B}) = -\frac{1}{|\mathcal{B}|}\sum_{\mathbf{S}_i\in\mathcal{B}} l(\hat{\mathbf{b}}_i, \mathbf{b}_i;\theta,\psi), \quad (3)$$

where $\mathcal{B}$ is a batch of samples, $l(\hat{\mathbf{b}}_i, \mathbf{b}_i;\theta,\psi)$ is the binary cross entropy loss given by

$$l(\hat{\mathbf{b}}_i, \mathbf{b}_i;\theta,\psi) = \sum_{k=1}^{K}[\mathbf{b}_i]_k \log_2(1-[\hat{\mathbf{b}}_i]_k) + (1-[\mathbf{b}_i]_k)\log_2([\hat{\mathbf{b}}_i]_k), \quad (4)$$

and $[\mathbf{b}_i]_k$ and $[\hat{\mathbf{b}}_i]_k$ denote the kth bit of the message and its estimate.

We use stochastic gradient descent (SGD) for training, where the vector of all trainable parameters $\phi^T = [\theta^T, \psi^T]$ is optimized in an iterative manner

$$\phi^{(t)} = \phi^{(t-1)} - \mu_t \nabla_\phi \mathcal{L}(\phi^{(t-1)}, \mathcal{B}^{(t)}), \quad (5)$$

where t is the iteration index, $\mu_t > 0$ is the learning rate, and $\mathcal{B}^{(t)}$ is a random batch from the dataset.

To ensure that the model is trained with many random realizations of the data and noise, we generate and use a new random set of samples in each epoch. We denote the dataset used in the u'th training epoch by $\mathcal{D}^u = \{\mathbf{S}_i\}_{i=1}^{|\mathcal{D}^u|}$, where $|\mathcal{D}^u| = \zeta|\mathcal{B}^u|$, ζ is a constant and $|\mathcal{B}^u|$ is the batch-size for the u'th epoch. Training DNNs with SGD, or its variants, requires careful choice of the training parameters (e.g., learning rate, batch-size, etc.).

A. Batch-size Adaptation

In training machine learning models, a static batch-size held constant throughout the training process forces the user to resolve a tradeoff. Small batch sizes are desirable since they tend to achieve faster convergence. On the other hand, large batch sizes offer more data-parallelism, which in turn improves computational efficiency and scalability. However, for the specific channel encoder/decoder training task a significantly larger batch size is necessary not only due to the data-parallelism benefits, but also because after a few training steps, the error rate and consequently the binary cross entropy loss (3) becomes very small, typically $10^{-4} \sim 10^{-7}$ for the range of SNR values considered here. Hence, to get a statistically accurate estimate of such a small loss value, and consequently, an accurate estimate of the gradient update in (5), the batch-size must be very large (typically ~ 10000 samples here).

We here propose an adaptive batch size scheme tailored for training a DNN-based channel encoder and decoder pair. In this scheme, we train the model starting from a small batch-size $|\mathcal{B}^1|$, and multiply the batch size by a factor of $\kappa > 1$ whenever the cross entropy loss does not decrease by a factor of λ in two consecutive epochs, until we reach a maximum batch-size of B_{max}. The maximum batch-size is constrained by the memory resources available to our training platform. We hence train with a sequence of batch-sizes, $|\mathcal{B}^1| \leq |\mathcal{B}^2| \leq \cdots \leq |\mathcal{B}^U| \leq B_{max}$, where U is the total number of epochs. Starting from a smaller batch size enables a faster convergence during initial epochs. We increase the batch size whenever trapped around a minimum due to insufficiency of the batch size to achieve an accurate estimate of the gradient. The proposed batch-size adaptation stabilizes and speeds up the training process.

B. SNR Scheduling

When training the channel encoder/decoder pair for a range of SNR values, if low and high SNR samples are presented to the decoder together during training, the trained DNN tends to be biased towards the lower SNR. This is because the error probability for higher SNR values can be orders of magnitude smaller than the lower ones. Hence, the contribution of the high SNR samples in the batch to the binary cross entropy loss (3) becomes negligible. In this case, the low SNR samples will decide the loss value and consequently the gradient updates (5) causing the channel code to be biased towards lower SNR values.

To train a channel encoder and decoder pair suitable for a wide SNR range, we here propose a scheduled-SNR training approach. This is motivated by the idea of curriculum training [18], [19], which suggests using a "curriculum" in presenting training samples to the DNN based on their "difficulty". Curriculum training improves both the speed of convergence of the training process, and the quality of the local minima obtained in the case of non-convex optimization criteria [18], [19]. Assume the goal is to efficiently train a channel encoder/decoder pair that works sufficiently well for all forward channel SNR values $\rho \in [\rho_{min}, \rho_{max}]$. We start training with lower SNR samples and increase the SNR along the epochs using a SNR schedule of $\rho_{min} = \rho_1 \leq \rho_2 \leq \cdots \leq \rho_U = \rho_{max}$. We observed that SNR scheduling combined with batch-size adaptation not only stabilizes and speeds up the training, but also improves the SNR-robustness when training an encoder/decoder pair for a wide SNR range.

V. Numerical Evaluations

In this section, we evaluate the performance of the proposed DRF codes and provide comparisons with previous works. In all the simulations, we use 10^9 random samples to achieve a reliable estimate of the error rate. Each sample includes a random realization of the message $\mathbf{b}$, and the corresponding random realizations of forward and feedback channels. We set $K = 50, L = 153$, and use the Adam optimizer. The values of the hyperparameters are: $U = 15$, $|\mathcal{B}^1| = 1000$, $B_{max} = 16000$, $\zeta = 100$, $\lambda = 2$, $\kappa = 2$.

A. AWGN Channel

We first consider a static AWGN channel, i.e. $\alpha_i = 1, \forall i$. We show the robustness of the proposed DRF codes to a mismatch between the training and the actual channel SNR values, and provide BLER comparisons with existing conventional and feedback channel codes. We show that the DRF codes outperform the benchmark low density parity check (LDPC) codes adopted for the fifth generation new radio (5G NR) [20], by three orders of magnitude and the previously proposed Deepcode [12] by an order of magnitude.

*1) **SNR-Robustness**:* We first compare the BLER of the proposed DRF codes with and without the attention module, when there is a mismatch between the actual channel SNR, ρ, and the SNR used for training, $\hat{\rho}$. Here, we train the codes with batch-size adaption but for a specific SNR value (i.e., without SNR scheduling). The SNR mismatch is defined as $\Delta\rho = \rho - \hat{\rho}$. The results are depicted in Fig. 3, where we plot BLER versus $\Delta\rho$ for $\rho = -1, 0, 1$ dB. This figure shows that without the SNR-aware attention module at the decoder, the BLER is very sensitive to the SNR mismatch. In this case, a negative SNR mismatch (i.e., training SNR is higher than the actual channel SNR), can significantly degrade the BLER by orders of magnitude. The BLER is less sensitive to a positive mismatch but still roughly an order of magnitude BLER degradation is observed if there is $\Delta\rho = +3$ dB mismatch between the training and test SNR values. This figure shows that DRF codes are significantly more robust to both positive and negative SNR mismatch due to the SNR-aware attention layers added to the decoder.

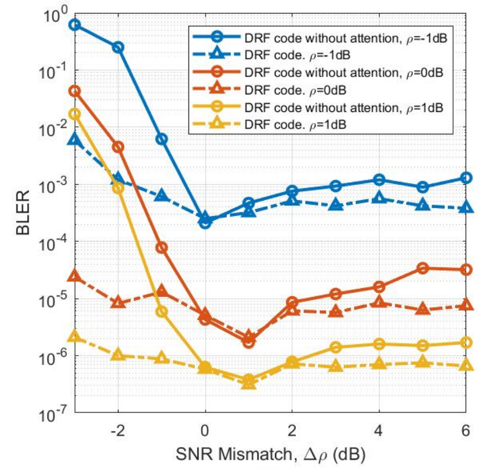

Fig. 3: Comparison between the DRF code and LSTM-based Deepcode in terms of BLER as a function of SNR mismatch $\Delta\rho$ (Noiseless feedback).

*2) **Comparison with Previous Works**:* In Fig. 4, we compare the performance of DRF codes with NR LDPC [20], Deepcode [12], and the DEF code [14]. We plot the BLER values achieved for each code for the forward channel SNR values in the range $[-1, 2]$ dB when (a) the feedback is noiseless ($\eta = \infty$), and (b) the feedback SNR is $\eta = 20$ dB. The blue curve reports the BLER for the RNN-based Deepcode architecture proposed in [12]. According to this figure, the proposed DRF codes reduce the BLER by almost three orders of magnitude in comparison with NR LDPC and an order of magnitude in comparison with Deepcode [12]. Note that for the Deepcode and DEF code, we have trained and used a different DNN for each of the four SNR points. However, for the DRF code, we have used a single DNN for all the SNR points, which is trained using our proposed SNR scheduling approach. Hence, in comparison with the state-of-the-art DEF code, DRF code achieves SNR-robustness with no significant performance degradation in the noiseless feedback case. When the feedback is noisy, DRF code also outperforms DEF code.

B. Fading Channel

In this subsection, we consider fading channels with feedback as depicted in Fig. 1. Depending on the wireless environment, the CSI coefficient α_i may follow various statistics. We adopt the Rayleigh fading channel model with an average power of $\Omega = 2\sigma^2$. In Fig. 5, we compare the resulting BER curves for DRF codes over both fast and slow Rayleigh fading channels depending on the availability of CSI at the receiver (CSIR). With CSIR, the decoder first performs LMMSE channel compensation on the received symbols, i.e., $\hat{y}_i = \frac{\alpha_i}{|\alpha_i|^2 + \sigma_n^2}$, and then uses $\hat{y}_i$ as input to the bi-directional LSTM units for decoding. Note that the encoder is the same as depicted in Fig. 2a for both cases. Fig. 5a exhibits the BER curves for the noiseless feedback case ($\eta = \infty$), and Fig. 5b for the noisy feedback case at $\eta = 20$dB. For a fair comparison, we use the exact value of α_i (not its estimate) both at the encoder and decoder. The curves show similar performance for the two cases with and without CSIR for both

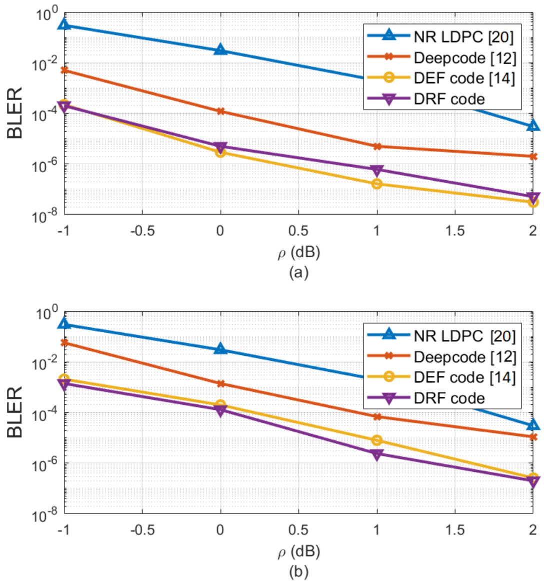

Fig. 4: Comparison between the proposed DRF codes and previous works, (a) Noiseless feedback, (b) Noisy feedback ($\eta = 20$dB).

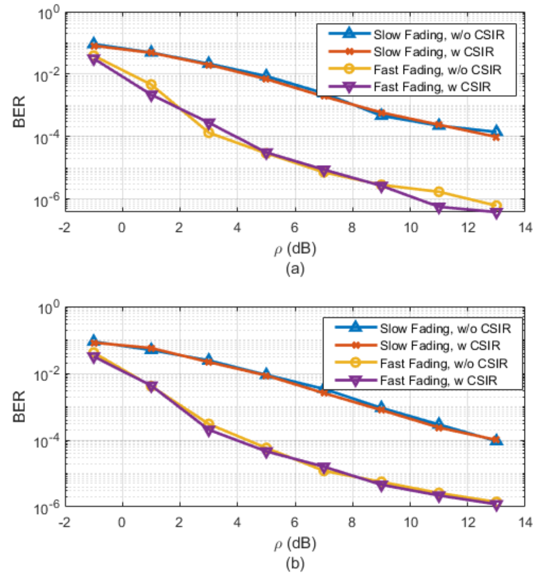

Fig. 5: The BER curves for DRF codes over Rayleigh magnitude fading channels with $\Omega = 1$ versus the average channel SNR, ρ (dB). (a) Noiseless feedback, (b) Noisy feedback ($\eta = 20$dB).

the slow and fast fading scenarios. In other words, the proposed DRF code learns to efficiently exploit the knowledge of the instantaneous CSI available at the transmitter through feedback, but no further improvement is achieved by providing the CSI also to the receiver. We believe that this is because the DRF code architecture inherently allows the receiver to adapt to the channel condition without a separate pilot transmission and channel estimation pipeline. This is a desirable property, which means that with the proposed DRF codes, the complexity and overhead associated with pilot transmission and channel estimation at the receiver can be reduced.

VI. Conclusions

We proposed a DNN-based error correction code for fading channels with output feedback, called the DRF code. It is shown that the DRF code significantly improves over the previously proposed DNN-based codes in terms of the error rate as well as robustness to varying SNR values for AWGN channels with feedback. Over fading channels, we showed that DRF codes can learn to efficiently use the knowledge of the instantaneous channel fading (available to the encoder through feedback) to reduce the overhead and complexity associated with channel estimation at the receiver.

References

[1] C. Shannon, "The zero error capacity of a noisy channel," *IRE Transactions on Information Theory*, vol. 2, no. 3, pp. 8–19, 1956.
[2] J. Schalkwijk and T. Kailath, "A coding scheme for additive noise channels with feedback–part I: No bandwidth constraint," *IEEE Transactions on Information Theory*, vol. 12, no. 2, pp. 172–182, 1966.
[3] R. G. Gallager and B. Nakiboğlu, "Variations on a theme by Schalkwijk and Kailath," *IEEE Transactions on Information Theory*, vol. 56, no. 1, pp. 6–17, 2010.
[4] Y. Polyanskiy, H. V. Poor, and S. Verdu, "Feedback in the non-asymptotic regime," *IEEE Transactions on Information Theory*, vol. 57, no. 8, pp. 4903–4925, 2011.
[5] J. Ooi and G. Wornell, "Fast iterative coding techniques for feedback channels," *IEEE Transactions on Information Theory*, vol. 44, no. 7, pp. 2960–2976, 1998.
[6] Z. Chance and D. J. Love, "Concatenated coding for the AWGN channel with noisy feedback," *IEEE Transactions on Information Theory*, vol. 57, no. 10, pp. 6633–6649, 2011.
[7] Z. Ahmad, Z. Chance, D. J. Love, and C.-C. Wang, "Concatenated coding using linear schemes for Gaussian broadcast channels with noisy channel output feedback," *IEEE Transactions on Communications*, vol. 63, no. 11, pp. 4576–4590, 2015.
[8] K. Vakilinia, S. V. S. Ranganathan, D. Divsalar, and R. D. Wesel, "Optimizing transmission lengths for limited feedback with nonbinary LDPC examples," *IEEE Transactions on Communications*, vol. 64, no. 6, pp. 2245–2257, 2016.
[9] Y. Kim, A. Lapidoth, and T. Weissman, "The Gaussian channel with noisy feedback," in *2007 IEEE International Symposium on Information Theory*, 2007, pp. 1416–1420.
[10] P. Elias, "Coding for noisy channels," *IRE Convention record*, vol. 4, pp. 37–46, 1955.
[11] A. Ben-Yishai and O. Shayevitz, "Interactive schemes for the AWGN channel with noisy feedback," *IEEE Transactions on Information Theory*, vol. 63, no. 4, pp. 2409–2427, 2017.
[12] H. Kim, Y. Jiang, S. Kannan, S. Oh, and P. Viswanath, "Deepcode: Feedback codes via deep learning," *IEEE Journal on Selected Areas in Information Theory*, vol. 1, no. 1, pp. 194–206, 2020.
[13] Y. Jiang, H. Kim, H. Asnani, S. Oh, S. Kannan, and P. Viswanath, "Feedback turbo autoencoder," in *IEEE International Conference on Acoustics, Speech and Signal Processing (ICASSP)*, 2020, pp. 8559–8563.
[14] A. R. Safavi, A. G. Perotti, B. M. Popovic, M. B. Mashhadi, and D. Gündüz, "Deep extended feedback codes," *ITU Journal on Future and Evolving Technologies (ITU J-FET)*, vol. 2, no. 6, pp. 33–41, 2021.
[15] Y. Kim, C. Denton, L. Hoang, and A. M. Rush, "Structured attention networks," in *5th International Conference on Learning Representations, ICLR 2017, Toulon, France, April 24-26, 2017, Conference Track Proceedings*, 2017.
[16] A. Vaswani, N. Shazeer, N. Parmar, J. Uszkoreit, L. Jones, A. N. Gomez, L. Kaiser, and I. Polosukhin, "Attention is all you need," in *Neural Information Processing Systems*, 2017.
[17] R. Jozefowicz, W. Zaremba, and I. Sutskever, "An empirical exploration of recurrent network architectures," in *Proceedings of the 32th International Conference on Machine Learning*, 2015, pp. 2342–2350.
[18] Y. Bengio, J. Louradour, R. Collobert, and J. Weston, "Curriculum learning," in *26th Annual International Conference on Machine Learning (ICML 2009)*, June 2009, pp. 41–48.
[19] A. Graves, M. G. Bellemare, J. Menick, R. Munos, and K. Kavukcuoglu, "Automated curriculum learning for neural networks," in *Proceedings of the 34th International Conference on Machine Learning*, 2017, pp. 1311–1320.
[20] Huawei-HiSilicon, "Performance evaluation of LDPC codes for NR eMBB data," *R1-1713740, 3GPP RAN1 meeting 90, Prague, Czech Republic*, August 21–25, 2017.